

# Particles confined in arbitrary potentials with a class of finite-range repulsive interactions

Avanish Kumar , Manas Kulkarni \*, and Anupam Kundu †

*International Centre for Theoretical Sciences, Tata Institute of Fundamental Research, Bengaluru 560089, India*



(Received 29 December 2019; accepted 19 August 2020; published 17 September 2020)

In this paper, we develop a large  $N$  field theory for a system of  $N$  classical particles in one dimension at thermal equilibrium. The particles are confined by an arbitrary external potential,  $V_{\text{ex}}(x)$ , and repel each other via a class of pairwise interaction potentials  $V_{\text{int}}(r)$  (where  $r$  is distance between a pair of particles) such that  $V_{\text{int}} \sim |r|^{-k}$  when  $r \rightarrow 0$ . We consider the case where every particle is interacting with  $d$  (finite-range parameter) number of particles to its left and right. Due to the intricate interplay between external confinement, pairwise repulsion, and entropy, the density exhibits markedly distinct behavior in three regimes  $k > 0$ ,  $k \rightarrow 0$ , and  $k < 0$ . From this field theory, we compute analytically the average density profile for large  $N$  in these regimes. We show that the contribution from interaction dominates the collective behavior for  $k > 0$  and the entropy contribution dominates for  $k < 0$ , and both contribute equivalently in the  $k \rightarrow 0$  limit (finite-range log-gas). Given the fact that this family of systems is of broad relevance, our analytical findings are of paramount importance. These results are in excellent agreement with brute-force Monte Carlo simulations.

DOI: [10.1103/PhysRevE.102.032128](https://doi.org/10.1103/PhysRevE.102.032128)

## I. INTRODUCTION

Systems of interacting particles confined in external potentials are ubiquitous in nature. Particularly, pairwise repulsive interactions with power-law divergences have taken a special place in physics and mathematics. There have been several theoretical investigations on such systems [1]. Examples include one-dimensional one-component plasma [2], one-dimensional Coulomb chains [3], Riesz gas [4–6], random matrix theory, nuclear physics, mesoscopic transport, quantum chaos, number theory [1,7–9], the Calogero-Moser model [10–15], dipolar gas confined to one dimension [16–19], and screened Coulomb or Yukawa gas [20,21] including finance [22] and big-data science [23]. A common feature that most of the above studies have is that the interaction among the particles is long ranged, which means every particle is interacting with every other particle in the system. Such interactions have led to developments of field theories which have been successfully used to understand various properties like density profiles, number fluctuations, level-spacing distributions, large deviations, etc., in equilibrium in the large  $N$  limit. In the context of integrable models, such field theories have also been used to understand nonequilibrium features such as shock waves and solitons [24–26].

In most physical systems, however, interaction between a pair of particles gets often screened, which essentially makes the interaction finite ranged. This naturally raises the following question: What are the effects of finite-ranged interactions on the field theory and the consequences stemming from it? In this paper, we precisely address this issue by studying a collection of  $N$  classical particles with positions  $\{x_i\}$  for  $i =$

$1, 2, \dots, N$  in a confining potential  $V_{\text{ex}}(x)$  in one dimension such that  $V_{\text{ex}}(x) \rightarrow \infty$  as  $|x| \rightarrow \infty$ . Each particle interacts with  $d$  particles on its right and left (if available) and does so via a repulsive interaction  $V_{\text{int}}(r)$  (where  $r$  is the distance between a pair of particles) such that  $V_{\text{int}} \sim |r|^{-k}$  when  $r \rightarrow 0$  for  $k > -k^*$  where  $k^*$  is the largest power in the Taylor series expansion of  $V_{\text{ex}}(r)$ . For  $k \leq -k^*$ , even the ground state (obtained from energy minimization) of the system is unstable because the particles fly off to  $x = \pm\infty$ . It is important to mention that recent cutting-edge developments in experiments have generated a lot of interest in such finite-ranged systems, e.g., cold atomic gases and ions [27], dipolar bosons [16–18,28], and Rydberg gases [29].

## II. MODEL AND PROPERTIES

The total energy of our system is given by

$$E(\{x_i\}) = \frac{1}{2} \sum_{i=1}^N V_{\text{ex}}(x_i) + \frac{J \operatorname{sgn}(k)}{2} \sum_{\substack{|i-j| \leq d \\ j \neq i}} V_{\text{int}}(|x_i - x_j|) \quad (1)$$

where  $J > 0$  and  $d$  is an integer. Note that the parameter  $d$  in Eq. (1) determines the number of particles that each particle is allowed to interact with. For example, by increasing the value of  $d$  from 1 to  $N - 1$ , one can go from nearest neighbor interaction to an all-to-all interaction scenario. This model is a generalization of the so-called Riesz gas [4]. Since we are interested in the equilibrium statistical properties of only the position degrees of freedom, the kinetic energy term in the Hamiltonian is omitted.

For the energy in Eq. (1), the equilibrium joint probability distribution function of the positions of the particles at finite temperature  $T = 1/\beta$  is given by

\*manas.kulkarni@icts.res.in

†anupam.kundu@icts.res.in

$P(x_1, \dots, x_N) = \frac{1}{Z_N(\beta)} e^{-\beta E[\{x_i\}]}$ , where the partition function  $Z_N(\beta) = \int \prod_{i=1}^N dx_i e^{-\beta E[\{x_i\}]}$ . While the confining potential tries to pull all the particles to its minimum, the pairwise repulsion as well as the entropy try to spread them apart. Because of this intricate competition, it turns out that the particles settle down over a finite region  $[-\ell_N, \ell_N]$  for  $k > 0$  and over the whole line for  $k \leq 0$  with an average macroscopic density  $\langle \hat{\rho}_N(x) \rangle = N^{-1} \sum_{i=1}^N \langle \delta(x - x_i) \rangle$ , where  $\langle \dots \rangle$  denotes an average with respect to the Boltzmann weight. An important question to ask is the following: What is the average density for large  $N$  and how does it depend on  $T$ ,  $k$ , and  $d$ ?

### III. KEY FINDINGS

In this paper, we address the question of average density for  $d \sim O(1)$  and find three distinct fascinating scenarios. We show that for  $k > 0$  the average density is obtained from a field theory where the interaction term dominates. On the other hand, for  $k < 0$  the entropy dominates. Remarkably, for  $k \rightarrow 0$ , both interaction and entropy contribute equivalently at finite temperature.

In particular, for an external potential of the polynomial form of  $n$ th order,  $V_{\text{ex}}(x_i) = \sum_{p=1}^n a_p x_i^p$ , we find that for  $k > 0$  the average density has the scaling form  $\langle \hat{\rho}_N(x) \rangle = \ell_N^{-1} f_k(x/\ell_N)$  in the large  $N$  limit where  $\ell_N = N^{\frac{k}{k+n}}$  and

$$f_k(y) = A_d(k)[2\mu_d(k) - V_{\text{ex}}(y)]^{1/k}, \quad \text{for } |y| \leq \Sigma[\mu_d(k)]. \quad (2)$$

The edge of the density  $\Sigma[\mu_d(k)]$  can be obtained from the real zero, closest to the origin, of the equation  $V_{\text{ex}}(y) = 2\mu_d(k)$  and  $A_d(k) = [2J\zeta_d(k)(k+1)]^{-\frac{1}{k}}$  with  $\zeta_d(k) = \sum_{n=1}^d n^{-k}$ . The function  $\mu_d(k)$  can then be determined by the normalization condition:

$$\int_{-\Sigma[\mu_d(k)]}^{\Sigma[\mu_d(k)]} f_k(y) dy = 1. \quad (3)$$

In order to make sure that all terms in the polynomial contribute on an equal footing, the coefficients themselves need to be scaled as  $a_p \sim N^{\frac{k}{k+n}(n-p)}$ . It is important to mention that external potentials in the form of polynomials are of relevance both experimentally as well as theoretically [30,31] and for such potentials we have  $k^* = n$ . Note that no such finite bound on  $k$  exists for those  $V_{\text{ex}}(x)$  which have infinite series representations, e.g., boxlike potentials such as  $V_{\text{ex}}(x) = a \cosh(bx)$  [26,32–36].

In the  $k < 0$  case, for any arbitrary external potential  $V_{\text{ex}}(x)$ , we find that the entropy term dominates to yield

$$f_k(y) = e^{-\beta V_{\text{ex}}(y)}/C, \quad \text{for } -\infty \leq y \leq \infty, \quad (4)$$

with  $\ell_N = 1$  (no scaling). The normalization constant  $C$  is fixed by  $\int_{-\infty}^{\infty} f_k(y) dy = 1$ .

The  $k \rightarrow 0$  limit turns out to be very interesting and subtle. To make sense of this limit, we choose  $V_{\text{int}}(r) = |r|^{-k}$ . Replacing  $\text{sgn}(k)$  in Eq. (1) by  $\pm 1$  for  $k \rightarrow 0^\pm$ , we use  $|r|^{-k} \approx 1 - k \log|r|$  and set  $J = 1/|k|$ . This up to an overall additive

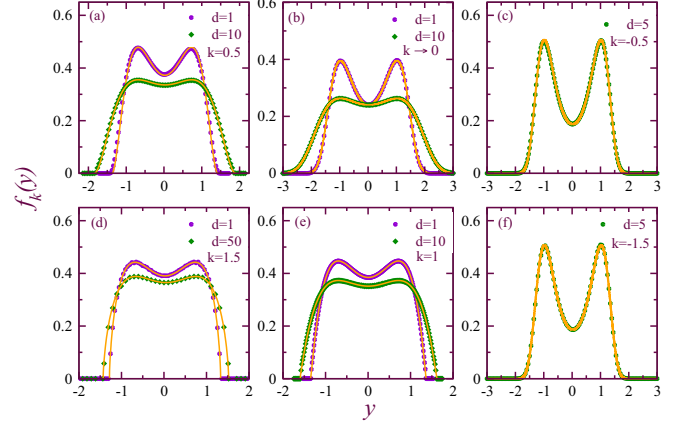


FIG. 1. Comparison of the densities with Monte Carlo simulation for different values of  $k$  and  $d$ . The external potential for all the plots is  $V_{\text{ex}}(x) = \frac{1}{2}(x^4 - N^{\frac{2k}{k+2}} x^2)$ . The interaction potential used in plots (a), (c), (d), (e), and (f) is  $V_{\text{int}}(r) = |r|^{-k}$  whereas in plot (b) it is  $V_{\text{int}}(r) = -\ln|r|$ . The solid lines in each plot are from theory and symbols are from numerical simulation. For plots with  $k > 0$  (a, d, e), the theoretical densities are given in Eq. (2). For the log-gas case (b),  $k \rightarrow 0$ , we compare simulation data with the analytical expression in Eq. (6). The plots (c) and (f) on the right column correspond to  $k < 0$  where we find the Boltzmann distribution given in Eq. (4). Excellent agreement is seen in all cases with no fitting parameters.

constant provides

$$E(\{x_i\}) = \frac{1}{2} \sum_{i=1}^N V_{\text{ex}}(x_i) - \frac{1}{2} \sum_{\substack{|i-j| \leq d \\ j \neq i}} \ln|x_i - x_j|. \quad (5)$$

We call this system the finite-range log-gas [37–39]. The  $k \rightarrow 0$  limit can also be taken for some other choices of  $V_{\text{int}}(r)$  such as  $1/|\sin(r)|^k$  and  $1/|\sinh(r)|^k$ , which yields generalized versions of the finite-range log-gas where the interaction term inside the summation becomes  $\ln|\sin(x_i - x_j)|$  and  $\ln|\sinh(x_i - x_j)|$ , respectively [1,7]. For all these cases, it turns out that, contributions from both interaction and entropy appear at the same order of  $N$  and one finally gets

$$f_k(y) = e^{-\frac{\beta V_{\text{ex}}(y)}{\beta d+1}}/C_0, \quad \text{for } -\infty \leq y \leq \infty \quad (6)$$

with  $\ell_N = 1$  and  $C_0$  being the normalization constant.

We also performed Monte Carlo (MC) simulations for several values of  $k$  and find excellent agreement with our analytical predictions (see Figs. 1 and 2). In what follows we discuss the derivation of the large  $N$  field theory and the saddle point calculations that lead to our results.

### IV. LARGE $N$ FIELD THEORY

We are interested to compute  $\langle \hat{\rho}_N(x) \rangle$  for large  $N$ , which is formally given by the following functional integral:

$$\langle \hat{\rho}_N(x) \rangle = \int \mathcal{D}[\rho(z)] \mathbb{P}[\hat{\rho}_N(z) = \rho(z)] \rho(x), \quad (7)$$

$\forall x$ , where  $\mathbb{P}$  represents the joint probability density functional (JPDF) that  $\hat{\rho}_N(z) = \rho(z)$ ,  $\forall z \in [-\infty, \infty]$ . The JPDF, for

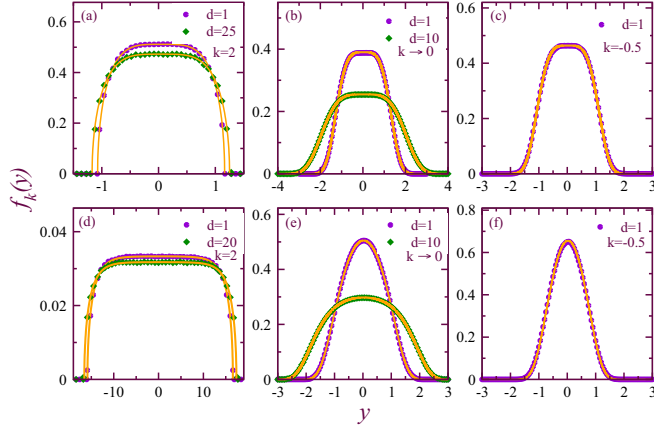


FIG. 2. Demonstration of the validity of our theoretical results in more general cases of interactions as well as external potentials. For the plots in the top row, the external potential is  $V_{\text{ex}}(x) = x^4/2$ . For the plots in the bottom row we have  $V_{\text{ex}}(x) = \frac{1}{2}\cosh(\frac{x}{2})$ , which naturally sets a  $N$  independent length scale, i.e.,  $\ell_N \sim O(1)$ , because it is not in the form of a finite-degree polynomial (diverges exponentially at  $|x| \rightarrow \infty$ ). The interaction potential used for the plots in the first column (a, d) is  $V_{\text{int}}(r) = \frac{1}{|\text{Sinh}(r)|^k}$  whereas in the second column (b, e) it is  $V_{\text{int}}(r) = \ln|\text{Sinh}(r)|$  and in the third column (c, f) it is  $V_{\text{int}}(r) = \sqrt{r} + \frac{r^{5/2}}{12}$  with  $r = |x_i - x_j|$ . The solid lines in each plot correspond to our theoretical results and the symbols are from numerical simulations. For plot (a), we find that the density is given by Eq. (2). In plot (d) we compare our simulation data with the analytical expression  $f_k(x) = C^{-1/k}[2\mu - N\cosh(x/2)]^{1/k}$  with  $C = 2J(k+1)\zeta_d(k)N^{k+1}$ , where  $\mu$  is fixed by normalization. The solid lines of the plots in the second and third columns are given in Eqs. (6) and (4), respectively. Once again we observe excellent agreement with no fitting parameters.

large  $N$ , can be written as

$$\begin{aligned} \mathbb{P}[\hat{\rho}_N(z) = \rho(z)] &= \frac{\int dx_1 \dots dx_N \delta[\hat{\rho}_N(z) - \rho(z)] e^{-\beta E(\{x_i\})}}{\int dx_1 \dots dx_N e^{-\beta E(\{x_i\})}} \\ &= \frac{\mathcal{J}_N[\rho(z)] e^{-\beta \mathcal{E}_N[\rho(z)]} \delta[\int \rho(z) dz - 1]}{\int \mathcal{D}[h(z)] \mathcal{J}_N[h(z)] e^{-\beta \mathcal{E}_N[h(z)]} \delta[\int h(z) dz - 1]} \end{aligned}$$

where we have assumed that for large  $N$  the energy in Eq. (1) can be expressed as a functional of the macroscopic density  $\hat{\rho}_N(z) = N^{-1} \sum_{i=1}^N \delta(z - x_i)$ , i.e.,  $E(\{x_i\}) \approx \mathcal{E}_N[\hat{\rho}_N(z)]$ . In fact this is shown explicitly below [after Eq. (13)]. The combinatorial factor  $\mathcal{J}_N[\rho(z)]$  counts the number of microscopic configurations compatible with given macroscopic profile  $\rho(z)$ . In fact  $\mathcal{J}_N[\rho(z)]$  is actually the exponential of the entropy associated to macroscopic density profile  $\rho(z)$  [40,41]:

$$\mathcal{J}_N[\rho(z)] = e^{-N \int dz \rho(z) \ln \rho(z)}. \quad (8)$$

The delta function  $\delta[\int \rho(z) dz - 1]$  ensures the normalization of the density functions. Replacing this normalization constraint by its integral representation  $\int \frac{d\mu}{2\pi} e^{-\mu w} = \delta(w)$  (where the integral is along the imaginary  $\mu$  axis)

we get

$$\begin{aligned} \mathbb{P}[\rho(z)] &= \frac{\int d\mu e^{-S_{N,\mu}[\rho(z)]}}{\int d\mu \int \mathcal{D}[h(z)] e^{-S_{N,\mu}[h(z)]}}, \quad \text{with} \quad (9) \\ S_{N,\mu}[\rho(z)] &= \beta \mathcal{E}_N[\rho(z)] + N \int dz \rho(z) \ln \rho(z) \\ &\quad + \mu \left[ \int \rho(z) dz - 1 \right]. \quad (10) \end{aligned}$$

We find (shown below) that the functional  $S_{N,\mu}[\rho(z)]$  for large  $N$  grows as  $N^{\gamma_k}$  with  $\gamma_k > 1$ . Hence the partition function in the denominator of Eq. (9) can be performed using saddle point method to give

$$\mathbb{P}[\rho(z)] \simeq \int d\mu e^{-\{S_{N,\mu}[\rho(z)] - S_{N,\mu^*}[\rho_N^*(z)]\}} \quad (11)$$

where  $\rho_N^*(z)$  and  $\mu^*$  are obtained by minimizing the action in Eq. (10) with respect to  $\rho(z)$  and  $\mu$ , i.e., solving the following equations:

$$\left. \frac{\delta S_{N,\mu}[\rho(z)]}{\delta \rho(z)} \right|_{\rho=\rho_N^*} = 0, \quad \text{with} \quad \int dz \rho_N^*(z) = 1. \quad (12)$$

Using the JPDF  $\mathbb{P}$  from Eq. (11) in Eq. (7) and again performing a saddle point integration for large  $N$  we find that the average density profile is the same as the most probable or the typical density profile, i.e.,

$$\langle \hat{\rho}_N(x) \rangle = \rho_N^*(x). \quad (13)$$

Next we compute the functional  $\mathcal{E}_N[\rho(z)]$  for the energy function given in Eq. (1). To do so we adapt the main idea of Ref. [5]. We first define a smooth function  $x(s)$  such that  $x(i) = x_i$ . This function  $x(s)$  becomes unique in the thermodynamic limit [25] and for a given density profile  $\rho(x)$  the position function  $x(i)$  is given explicitly by

$$i = N \int_{-\infty}^{x(i)} dz \rho(z). \quad (14)$$

Taking the single derivative with respect to  $x$  on both sides, we get  $di/dx = N\rho(x)$ , using which it is easy to see that for any smooth function  $g(x_i)$  of the coordinate  $x_i$

$$\sum_i g(x_i) = N \int dx g(x) \rho(x). \quad (15)$$

This can be directly applied to the external potential term in Eq. (1) to get  $\mathcal{E}_N^{\text{ex}}[\rho(x)] = (N/2) \int dx V_{\text{ex}}(x) \rho(x)$ . Expressing the interaction term in terms of the density profile  $\rho(x)$  is far from obvious and is discussed below. Using Eq. (14), we write the interaction term in Eq. (1) as  $\mathcal{E}_{\text{int}} = \sum_i \sum_j V_{\text{int}}[|i-j|x'(i) + \dots]$  where we have used the Taylor series expansion  $x(j) = x(i) + (j-i)x'(i) + \dots$ . Assuming  $x'(i)$  is small in the large  $N$  limit (see Appendices) and using  $V_{\text{int}}(r)|_{r \rightarrow 0} \sim |r|^{-k}$  we get  $\mathcal{E}_{\text{int}} = \frac{J \zeta_d(k) \text{sgn}(k)}{2} \sum_i [x'(i)]^{-k}$  where we have neglected the higher order terms in the Taylor series expansion as they are subleading. Now inserting  $x'(i) = 1/[N\rho(x)]$  and using Eq. (15) we have

$$\mathcal{E}_{\text{int}} = J \zeta_d(k) \text{sgn}(k) N^{k+1} \int dx \rho^{k+1}(x). \quad (16)$$

Hence the total energy functional  $\mathcal{E}_N = \mathcal{E}_{\text{ex}} + \mathcal{E}_{\text{int}}$  is given by

$$\mathcal{E}_N[\rho(x)] = \frac{N}{2} \int dx V_{\text{ex}}(x)\rho(x) + J \zeta_d(k) \text{sgn}(k) N^{k+1} \int dx \rho^{k+1}(x). \quad (17)$$

Following the same procedure it is possible to show from Eq. (5) that in the  $k \rightarrow 0$  limit one gets

$$\mathcal{E}_N[\rho(x)] = \frac{N}{2} \int dx V_{\text{ex}}(x)\rho(x) + Nd \int dx \rho(x) \ln \rho(x). \quad (18)$$

This result can also be obtained directly from Eq. (17) in the  $k \rightarrow 0$  limit after setting  $J = 1/|k|$ . We now discuss the three regimes separately.

## V. DISCUSSIONS

### A. Regime 1: $k > 0$

Inserting the above expression of the energy functional in Eq. (10), we observe that in the leading order one can neglect the entropy contribution [42]. For an external potential of  $n$ th order polynomial form, minimizing this action one finds that  $\langle \hat{\rho}_N(x) \rangle = \rho_N^*(x) = \ell_N^{-1} f_k(x/\ell_N)$  with  $\ell_N = N^{\frac{k}{k+n}}$  and  $f_k(y)$  given in Eq. (2). This result is verified numerically. Using this scaling form of the density in the action in Eq. (10), it is easy to see that  $\mathcal{S}_{N,\mu^*} \sim N^{\gamma_k}$  with  $\gamma_k = \frac{k(n+1)+n}{k+n}$ . In fact, for  $k > 1$ , the formula in Eq. (2) holds for any  $d$  even when  $d = N - 1$ , for which  $\zeta_d(k)$  becomes the usual Riemann zeta function  $\zeta(k)$ . This happens because, for  $k > 1$ , the contribution from all-to-all interaction comes only at  $O(N^2)$ , which is still subdominant [5]. It is to be noted that the above analysis fails for very high temperatures of the order  $\approx O(N^{-\frac{2k}{k+n}})$  when entropy becomes important. In the special case of a quadratic potential (i.e.,  $n = 2$  with  $a_1 = 0$  and  $a_2 = 1$ ), we get the following result for the support:  $\mu_d(k) = \frac{1}{8}[A_d(k)B(1 + 1/k, 1 + 1/k)]^{-\frac{2k}{k+2}}$  and  $\Sigma[\mu_d(k)] = \sqrt{2\mu_d(k)}$ .

### B. Regime 2: $k < 0$

In this regime, interestingly, as pairwise interaction is of  $O(N^{1-|k|})$ , it becomes irrelevant in comparison to the entropy term, which is of  $O(N)$ . Therefore, minimizing the action, which now involves only the external potential and entropy, gives us the usual Boltzmann distribution in Eq. (4) with  $\ell_N = 1$  for any external potential. It is noteworthy that the density profile becomes independent of the details of the interaction although it plays an important role to have a description in terms of macroscopic particle densities.

### C. Regime 3: $k \rightarrow 0$

In the case of finite-range log-gas, as can be seen using Eq. (18) in Eq. (10), there is an intricate interplay between pairwise interaction and entropy because they contribute at the same order. Minimizing this action Eq. (10), we get Eq. (6) for any external potential. This result was also recently obtained via a microscopic method [38]. Interaction energy and entropy

contributing equivalently has also been observed in log-gas with all-to-all interactions [43,44].

## VI. NUMERICAL METHOD AND DETAILS

Our analytical predictions were tested against brute-force MC simulations for  $N = 501$  and  $\beta = 1$ . In our simulations we collect data after every ten MC cycles and averages were performed over around  $10^7$ – $10^8$  samples to compute the particle densities in different cases discussed above. We compare these results with our theoretical expression in Figs. 1 and 2 and observe excellent agreement in all cases. To make sure that we collect data after the system has relaxed to an equilibrium state, we checked for the equipartition by computing virial  $\langle x_j \frac{\partial E(\{x_j\})}{\partial x_j} \rangle$ . The excellent agreement with the equipartition, thereby benchmarking our numerics, is given in the Appendices.

## VII. CONCLUSIONS AND OUTLOOK

In this paper, we derive a large  $N$  field theory for a system of  $N$  particles repulsively interacting over a finite range and confined in arbitrarily external potentials. We discuss a family of interaction potentials  $V_{\text{int}}(r)$  such that they behave as  $\approx 1/|r|^k$  for small  $r$ . We identify three distinct regimes depending on the value of  $k$  and for each regime we derive the action in the large  $N$  limit. Minimizing this action provides us explicit expressions of the densities in arbitrary confining potentials. Our analytical results of densities are in excellent agreement with our brute-force numerical simulations. It is pertinent to mention that such densities of finite-ranged systems can be experimentally observed in a broad range of experiments such as ions [45,46] and dusty plasma [47] to name a few. This paper is of paramount importance since it is essentially a starting point for any analysis on a broad class of interacting classical systems. For example, if one wants to study nonlinear hydrodynamics [48,49], interacting overdamped Langevin particles [50], single-file motion [51], or large deviations [40,41,52,53] then writing a large  $N$  field theory is the very beginning step and a correct form of the energy functional is crucial.

Our paper paves the path for several future studies such as nontrivial extension to higher dimensions, extreme value statistics, level spacing distributions (i.e., statistics of gaps between successive particles), and large deviation functions of these externally confined pairwise interacting particles. Our paper acts as a genesis and provides a foundation for embarking in these exciting directions. Furthermore, the connection between these models and random matrix theories remains an open and interesting question. Finally, it would also be interesting to understand the crossover from finite-ranged interaction to all-to-all coupling [5].

## ACKNOWLEDGMENTS

M.K. would like to acknowledge support from the Indo-French Centre for the Promotion of Advanced Research (IFCPAR Project No. 6004-1), a Ramanujan Fellowship (Grant No. SB/S2/RJN-114/2016), a SERB Early Career Research Award (Grant No. ECR/2018/002085), and



a Matrics grant (Grant No. MTR/2019/001101) from the Science and Engineering Research Board, Department of Science and Technology, Government of India. A.K. would like to acknowledge support from IFCPAR (Project No. 5604-2) and a SERB Early Career Research Award (Grant No. ECR/2017/000634) from the Science and Engineering Research Board, Department of Science and Technology, Government of India. We gratefully acknowledge Hemanta Kumar G. and the ICTS-TIFR high performance computing facility.

#### APPENDIX A: CONTINUUM APPROXIMATION FOR THE FINITE-RANGE INTERACTION TERM

In Eq. (1) of the main text, we defined the energy of a microscopic configuration  $\{x_i\}$  as

$$E(\{x_i\}) = \frac{1}{2} \sum_{i=1}^N V_{\text{ex}}(x_i) + \frac{J \text{sgn}(k)}{2} \sum_{\substack{|i-j| \leq d \\ j \neq i}} V_{\text{int}}(|x_i - x_j|), \quad (\text{A1})$$

where  $J > 0$  and  $d$  is an integer. We want to express the interaction term

$$\mathcal{E}_{\text{int}} = \frac{J \text{sgn}(k)}{2} \sum_{\substack{|i-j| \leq d \\ j \neq i}} V_{\text{int}}(|x_i - x_j|)$$

as a functional of the macroscopic density  $\rho(z)$ . As noted in the main text, for large  $N$  one can define a smooth function  $x(i)$  such that

$$i = N \int_{-\infty}^{x(i)} dz \rho(z). \quad (\text{A2})$$

Using this equation, we can write

$$\mathcal{E}_{\text{int}} = \frac{J \text{sgn}(k)}{2} \sum_{\substack{|i-j| \leq d \\ j \neq i}} V_{\text{int}} \left[ \left| \sum_{n=1}^{\infty} \frac{(i-j)^n}{n!} x^{[n]}(i) \right| \right], \quad (\text{A3})$$

where  $x^{[n]}(i) = \frac{d^n x(i)}{d^i}$ . It easy to see (also justified later) that  $\frac{|x^{[n+1]}(i)|}{|x^{[n]}(i)|} \sim O(1/N)$ . Hence keeping only the leading order term in the Taylor series expansion in the argument of  $V_{\text{int}}$  we have

$$\begin{aligned} \mathcal{E}_{\text{int}} &\sim \frac{J \text{sgn}(k)}{2} \sum_{i=1}^N \sum_{\substack{|i-j| \leq d \\ j \neq i}} V_{\text{int}}[|i-j|x^{[1]}(i)|] \\ &\sim \frac{J \text{sgn}(k)}{2} \sum_{i=1}^N \sum_{\substack{|i-j| \leq d \\ j \neq i}} V_{\text{int}} \left( \frac{|i-j|}{N \rho[x(i)]} \right), \end{aligned}$$

$$\begin{aligned} \text{using } x^{[1]}(i) &= \frac{1}{N \rho[x(i)]} \\ &\sim \frac{J \text{sgn}(k)}{2} \sum_{i=1}^N \sum_{\substack{|i-j| \leq d \\ j \neq i}} \frac{N^k \rho[x(i)]^k}{|i-j|^k}. \quad (\text{A4}) \end{aligned}$$

In the last step we used the fact that  $x^{[1]}(i)$  is small, which is because of the following. We expect that  $\rho(x)$  should have the following scaling form:

$$\rho(x) = \frac{1}{\ell_N} f\left(\frac{x}{\ell_N}\right), \quad \text{with } \lim_{N \rightarrow \infty} \frac{\ell_N}{N} \rightarrow 0. \quad (\text{A5})$$

Assuming that the limit in Eq. (A5) is true we proceed and compute  $\rho(x)$  performing the action minimization procedure explained in the main text and finally check that this assumption is indeed true—thereby making the whole argument self-consistent.

Simplifying Eq. (A4) further we get

$$\begin{aligned} \mathcal{E}_{\text{int}} &\sim \frac{J \text{sgn}(k)}{2} \sum_{i=1}^N N^k \rho[x(i)]^k \sum_{\substack{|i-j| \leq d \\ j \neq i}} \frac{1}{|i-j|^k} \\ &\sim \frac{J \text{sgn}(k)}{2} \sum_{i=1}^N N^k \rho[x(i)]^k \sum_{n=1}^d \frac{1}{n^k} \\ &\sim J \text{sgn}(k) \zeta_d(k) \sum_{i=1}^N N^k \rho[x(i)]^k \\ &\sim J \text{sgn}(k) \zeta_d(k) N^{k+1} \int dx \rho(x)^{k+1}, \end{aligned}$$

$$\text{using } \sum_i g(x_i) = N \int dx g(x) \rho(x). \quad (\text{A6})$$

The above calculation is true for  $k > -k^*$  (see main text). However, for  $k \rightarrow 0$  (finite-range log-gas) the above expression gets simplified as follows: Setting  $J = 1/|k|$  and writing  $[N \rho(x)]^k = e^{k \ln[N \rho(x)]}$  and finally taking the  $k \rightarrow 0$  limit, we obtain

$$\mathcal{E}_{\text{int}} \sim d N \int dx \rho(x) \ln \rho(x) \quad (\text{A7})$$

up to an overall additive constant where we have used  $\zeta_d(0) = d$ . Now adding this functional form of  $\mathcal{E}_{\text{int}}[\rho(z)]$  to  $\mathcal{E}_{\text{ex}}[\rho(z)]$  we get the total energy functional  $\mathcal{E}_N[\rho(z)]$  for  $k \neq 0$ :

$$\begin{aligned} \mathcal{E}_N[\rho(x)] &= \frac{N}{2} \int dx V_{\text{ex}}(x) \rho(x) \\ &\quad + J \zeta_d(k) \text{sgn}(k) N^{k+1} \int dx \rho^{k+1}(x). \quad (\text{A8}) \end{aligned}$$

Following a similar calculation one can show that the energy functional for  $k \rightarrow 0$  becomes

$$\mathcal{E}_N[\rho(x)] = \frac{N}{2} \int dx V_{\text{ex}}(x) \rho(x) + Nd \int dx \rho(x) \ln \rho(x). \quad (\text{A9})$$

Inserting these expressions of the energy functionals in the expression of the action  $S_{N,\mu}[\rho(z)]$  below,

$$\begin{aligned} S_{N,\mu}[\rho(z)] &= \beta \mathcal{E}_N[\rho(z)] + N \int dz \rho(z) \ln \rho(z) \\ &\quad + \mu \left[ \int \rho(z) dz - 1 \right], \quad (\text{A10}) \end{aligned}$$

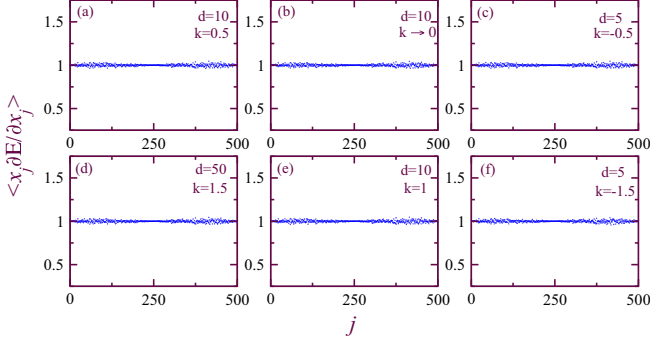


FIG. 3. Virial plots obtained from Eq. (B1) for the corresponding plots in Fig. 1.

and minimizing it we get the following saddle point equations:

$$\frac{1}{2}V_{\text{ex}}(x) + J(k+1)\zeta_d(k)\text{sgn}(k)N^k\rho^k(x) + \mu = 0, \quad \text{for } k > 0, \quad (\text{A11})$$

$$\frac{1}{2}V_{\text{ex}}(x) + (\beta d + 1)[\ln \rho(x) - 1] + \mu = 0, \quad \text{for } k = 0, \quad (\text{A12})$$

$$\frac{1}{2}V_{\text{ex}}(x) + [\ln \rho(x) - 1] + \mu = 0, \quad \text{for } k < 0, \quad (\text{A13})$$

in the leading order in  $N$ . Solving these equations we find that the saddle point density is given by Eq. (A5) with

$$\ell_N = \begin{cases} N^{\frac{k}{k+n}}, & \text{for } k > 0 \\ 1, & \text{for } k \leq 0 \end{cases} \quad (\text{A14})$$

and

$$f_k(y) = \begin{cases} A_d(k)[2\mu_d(k) - V_{\text{ex}}(y)]^{1/k}, & |y| \leq \Sigma[\mu_d(k)], \\ & \text{for } k > 0, \\ e^{-\frac{\beta V_{\text{ex}}(y)}{\beta d + 1}}/C_0, & -\infty \leq y \leq \infty, \\ & \text{for } k = 0, \\ e^{-\beta V_{\text{ex}}(y)}/C, & -\infty \leq y \leq \infty, \\ & \text{for } k < 0 \end{cases}$$

as announced in Eqs. (2), (4), and (6) in the main text. Here  $C$  and  $C_0$  are normalization constants. This clearly justifies the limit in Eq. (A5). It is easy to see that for boxlike potentials this limit is trivially true since there is a length scale set by the potential itself.

It is important to note that Eq. (A14) holds only when the system is stable and there is a notion of a density profile, i.e.,

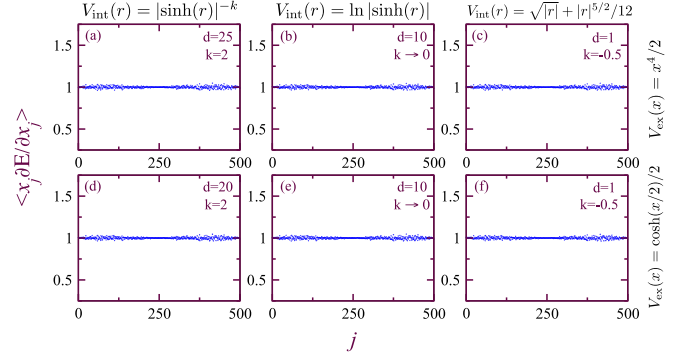


FIG. 4. Virial plots obtained from Eq. (B1) for the corresponding plots in Fig. 2.

Eq. (A5). The most suitable way to visualize this is as follows. If  $k < k^*$ , then even for a finite number of particles  $N$  there is no finite solution for the particle positions that minimize the energy in Eq. (A1). All particles in such a scenario fly away to  $\pm\infty$ , making the discussion on density void.

## APPENDIX B: VIRIALS (EQUIPARTITION)

To make sure that we collect data after the system has relaxed to the equilibrium state, we checked for the equipartition by computing virial  $\langle x_j \frac{\partial E(\{x_i\})}{\partial x_j} \rangle$ . Below we show the virials for all the plots in Figs. 1 and 2 in the main text. The equipartition was tested by checking that

$$\left\langle x_j \frac{\partial E(\{x_i\})}{\partial x_j} \right\rangle = k_B T. \quad (\text{B1})$$

Figures 3 and 4 show remarkable agreement, thereby validating all our numerical results.

Note that for  $k > 0$  when  $T \sim O(1)$  the finite temperature results match with the density profile obtained by minimizing the total energy Eq. (1) in the main text. In other words, we have  $N$  equations  $\frac{\partial E(\{x_i\})}{\partial x_i} = 0$ ,  $i = 1, 2, \dots, N$  from which we can solve for  $N$  unknowns  $\{x_i^{\text{min}}; i = 1, 2, \dots, N\}$ . Reconstructing a density function from this (say, by using the inverse of interparticle distance) will give a density profile which also will agree with the one obtained from minimization of the action described above. This in turn is in perfect agreement with brute-force finite temperature Monte Carlo. Needless to mention, this of course does not encode any information about fluctuations.

[1] P. J. Forrester, *Log-Gases and Random Matrices* (Princeton University, Princeton, NJ, 2010).  
 [2] A. Dhar, A. Kundu, S. N. Majumdar, S. Sabhapandit, and G. Schehr, *Phys. Rev. Lett.* **119**, 060601 (2017).  
 [3] D. H. E. Dubin, *Phys. Rev. E*, **55**, 4017 (1997).  
 [4] M. Riesz, *Acta Sci. Math. Univ. Szeged* **9**, 1 (1938).  
 [5] S. Agarwal, A. Dhar, M. Kulkarni, A. Kundu, S. N. Majumdar, D. Mukamel, and G. Schehr, *Phys. Rev. Lett.* **123**, 100603 (2019).  
 [6] D. P. Hardin, T. Leblé, E. B. Saff, and S. Serfaty, *Constr. Approx* **48**, 61 (2018).

[7] M. L. Mehta, *Random Matrices* (Academic, New York, 2004).  
 [8] *The Oxford Handbook of Random Matrix Theory*, edited by G. Akemann, G. Baik, and P. Di Francesco (Oxford University, London, 2011).  
 [9] G. Livan, M. Novaes, and P. Vivo, *Introduction to Random Matrices: Theory and Practice* (Springer, New York, 2018).  
 [10] F. Calogero, *J. Math. Phys.* **10**, 2197 (1969).  
 [11] F. Calogero, *J. Math. Phys.* **12**, 419 (1971).  
 [12] F. Calogero, *Lett. Nuovo Cimento* **13**, 411 (1975).  
 [13] J. Moser, in *Surveys in Applied Mathematics* (Elsevier, Amsterdam, 1976), pp. 235–258.

- [14] F. Calogero, *J. Math. Phys.* **22**, 919 (1981).
- [15] A. P. Polychronakos, *J. Phys. A: Math. Gen.* **39**, 12793 (2006).
- [16] M. Lu, N. Q. Burdick, S. H. Youn, and B. L. Lev, *Phys. Rev. Lett.* **107**, 190401 (2011).
- [17] A. Griesmaier, J. Werner, S. Hensler, J. Stuhler, and T. Pfau, *Phys. Rev. Lett.* **94**, 160401 (2005).
- [18] A. Griesmaier, J. Stuhler, T. Koch, M. Fattori, T. Pfau, and S. Giovanazzi, *Phys. Rev. Lett.* **97**, 250402 (2006).
- [19] K.-K. Ni, S. Ospelkaus, D. Wang, G. Quéméner, B. Neyenhuis, M. De Miranda, J. Bohn, J. Ye, and D. Jin, *Nature (London)* **464**, 1324 (2010).
- [20] F. D. Cunden, P. Facchi, M. Ligabò, and P. Vivo, *J. Stat. Mech.* (2017) 053303.
- [21] F. D. Cunden, P. Facchi, M. Ligabò, and P. Vivo, *J. Phys. A: Math. Theor.* **51**, 35LT01 (2018).
- [22] J.-P. Bouchaud and M. Potters, in *The Oxford Handbook of Random Matrix Theory*, edited by G. Akemann, J. Baik, and P. Di Francesco (Oxford University, New York, 2015).
- [23] R. C. Qiu and P. Antonik, *Smart Grid Using Big Data Analytics: A Random Matrix Theory Approach* (Wiley, New York, 2017).
- [24] A. G. Abanov, A. Gromov, and M. Kulkarni, *J. Phys. A: Math. Theor.* **44**, 295203 (2011).
- [25] M. Kulkarni and A. P. Polychronakos, *J. Phys. A: Math. Theor.* **50**, 455202 (2017).
- [26] A. K. Gon and M. Kulkarni, *J. Phys. A: Math. Theor.* **52**, 415201 (2019).
- [27] J. M. Brown and A. Carrington, *Rotational Spectroscopy of Diatomic Molecules* (Cambridge University, Cambridge, England, 2003).
- [28] Y. Tang, W. Kao, K.-Yu. Li, S. Seo, K. Mallayya, M. Rigol, S. Gopalakrishnan, and B. L. Lev, *Phys. Rev. X* **8**, 021030 (2018).
- [29] M. P. A. Jones, L. G. Marcassa, and J. P. Shaffer, *J. Phys. B* **50**, 060202 (2017).
- [30] A. P. Polychronakos, *Phys. Lett. B* **276**, 341 (1992).
- [31] B. M. Garraway and H. Perrin, *J. Phys. B* **49**, 172001 (2016).
- [32] A. P. Polychronakos, *Phys. Lett. B* **277**, 102 (1992).
- [33] A. L. Gaunt, T. F. Schmidutz, I. Gotlibovych, R. P. Smith, and Z. Hadzibabic, *Phys. Rev. Lett.* **110**, 200406 (2013).
- [34] T. F. Schmidutz, I. Gotlibovych, A. L. Gaunt, R. P. Smith, N. Navon, and Z. Hadzibabic, *Phys. Rev. Lett.* **112**, 040403 (2014).
- [35] N. Navon, A. L. Gaunt, R. P. Smith, and Z. Hadzibabic, *Science* **347**, 167 (2015).
- [36] S. J. Garratt, C. Eigen, J. Zhang, P. Turzák, R. Lopes, R. P. Smith, Z. Hadzibabic, and N. Navon, *Phys. Rev. A* **99**, 021601(R) (2019).
- [37] A. Pandey, A. Kumar, and S. Puri, *Phys. Rev. E* **96**, 052211 (2017).
- [38] A. Pandey, A. Kumar, and S. Puri, *Phys. Rev. E* **101**, 022217 (2020).
- [39] A. Kumar, A. Pandey, and S. Puri, *Phys. Rev. E* **101**, 022218 (2020).
- [40] D. S. Dean and S. N. Majumdar, *Phys. Rev. Lett.* **97**, 160201 (2006).
- [41] D. S. Dean and S. N. Majumdar, *Phys. Rev. E* **77**, 041108 (2008).
- [42] R. Lahiri, M. Barma, and S. Ramaswamy, *Phys. Rev. E* **61**, 1648 (2000).
- [43] R. Allez, J.-P. Bouchaud, and A. Guionnet, *Phys. Rev. Lett.* **109**, 094102 (2012).
- [44] R. Allez, J.-P. Bouchaud, S. N. Majumdar, and P. Vivo, *J. Phys. A: Math. Theor.* **46**, 015001 (2013).
- [45] Zhang, Jiehang, G. Pagano, P. W. Hess, A. Kyprianidis, P. Becker, H. Kaplan, A. V. Gorshkov, Z.-X. Gong, and C. Monroe, *Nature (London)* **551**, 601 (2017).
- [46] L. L. Yan, W. Wan, L. Chen, F. Zhou, S. J. Gong, X. Tong, and M. Feng, *Sci. Rep.* **6**, 21547 (2016).
- [47] B. A. Klumov, *JETP Lett.* **110**, 715 (2019).
- [48] M. Kulkarni and A. G. Abanov, *Phys. Rev. A* **86**, 033614 (2012).
- [49] H. Spohn, *J. Stat. Phys.* **154**, 1191 (2014).
- [50] D. S. Dean, *J. Phys. A: Math. Gen.* **29**, L613 (1996).
- [51] V. Démery, O. Bénichou, and H. Jacquin, *New J. Phys.* **16**, 053032 (2014).
- [52] A. Kundu and J. Cividini, *Europhys. Lett.* **115**, 54003 (2016).
- [53] A. Dhar, A. Kundu, S. N. Majumdar, S. Sabhapandit, and G. Schehr, *J. Phys. A: Math. Theor.* **51**, 295001 (2018).